False Bay Physical Oceanography Literature Review

CONTENTS

1 HISTORY OF FALSE BAY

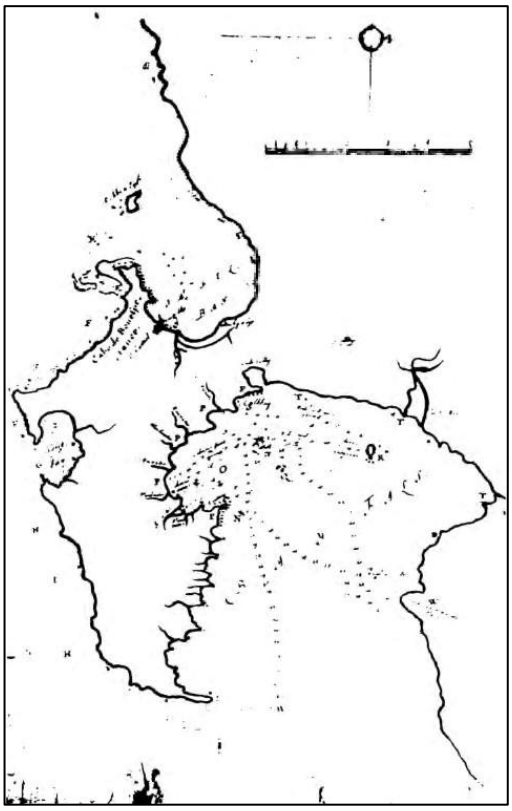

Figure 1) Map of False Bay and the Cape Peninsula drawn by Simon van der Stel in 1687 (From Gründlingh and Largier, 1988).

The Cape of Good Hope (Cape Point) is one of the most distinguished capes in maritime history and was first named *Cabo das tempestades (Cape of Storms)* by the Portuguese explorer Bartolomeu Dias in 1488 (Burman, 1977). Later, King John II of Portugal renamed it *Cabo de Boa Esperanza* "Cape of Good Hope" to reflect the optimism about a new sea route to the East (Burman, 1977). The establishment of a new trade route caused an influx of ship traffic around the Point

Heedless sailors mistook Cape Hangklip for Cape Point while sailing westward on their journey back to Europe. These unfortunate men found themselves in the bay with no northward thoroughfare. Following from this, the second cape to the east (Cape Hangklip) was called *Cabo Falso* (the false cape). Hence the bay was known as *Golfo de Falso,* and the first description of the bay was given by Antonio de Saldanha in 1503, after which it appeared on world maps (Burman, 1977).

The history of False Bay is far too long to attempt to summarise here. Shell middens near the northwestern shores bear evidence that Khoisan hunter-gatherers have exploited the bay for over 10 000 years' (Goodwin and Peers, 1953). The first maritime campaign to chart False Bay was attempted in 1672 by the crew of a Dutch warship, *Goudvinck* (Gründlingh and Largier, 1988). This was unsuccessful, as the ship was called to wage war with England and France. Simon van der Stel, the first governor of the former Dutch Cape Colony, recorded the depth measurements of False Bay onboard *De Noord* in 1687 (Gründlingh and Largier, 1988). The rough chart by the governor is included (Fig. 1).

2 SURROUNDING WATERS – REGIONAL INFLUENCES

Cape Point, and by extension False Bay, forms the western extremity of the Western Agulhas Bank (WAB) (Isaac, 1937; Largier et al., 1992). The WAB is a transitional shelf region which has been divided into three subregions by Largier et al. (1992), namely the coastal region, the mid-shelf region, and the shelf-edge region. The lack of correlation between currents and temperatures, found during the Western Agulhas Shelf Processes (WASP) experiments, in these subregions suggests that they function somewhat independently (Largier et al., 1992).

The shelf narrows dramatically toward Cape Point, and the coastal and shelf-edge frontal systems merge and are observed as an intense front and jet named the Good Hope Jet (Bang and Andrews, 1974). A set of boundary conditions must operate near the mouth of the bay, especially near Cape Point (Largier et al., 1992). At its mouth, the bay is exposed to the open ocean and WAB processes, which will be combined with the effect of the local wind to force the circulation in False Bay (Wainman et al., 1987)

Conditions in False Bay vary from wind-driven upwelling typical of the southwest coast to warm water intrusions from the Agulhas Current off the Agulhas Bank to the southeast (Isaac, 1937; Largier et al., 1992; Pfaff et al., 2019).

3 PHYSICAL CHARACTERISTICS OF FALSE BAY

3.1 BATHYMETRY AND SURROUNDING TOPOGRAPHY

False Bay is a square-shaped embayment on the southwest coast of South Africa. The central coordinates of the bay, as presented by Flemming (2024), are $34°14.0'S$ and $18°39.0'E$ (Figure 1). The maximum meridional extension of the bay is ~35 km from northern shore to the latitude crossing Cape Hangklip to the south $(34°23'S)$, while the zonal counterpart is ~39 km between Fish Hoek and Gordon's Bay (Flemming, 2024). The embayed area is approximately $1130\ km^2$ (Flemming, 2024).

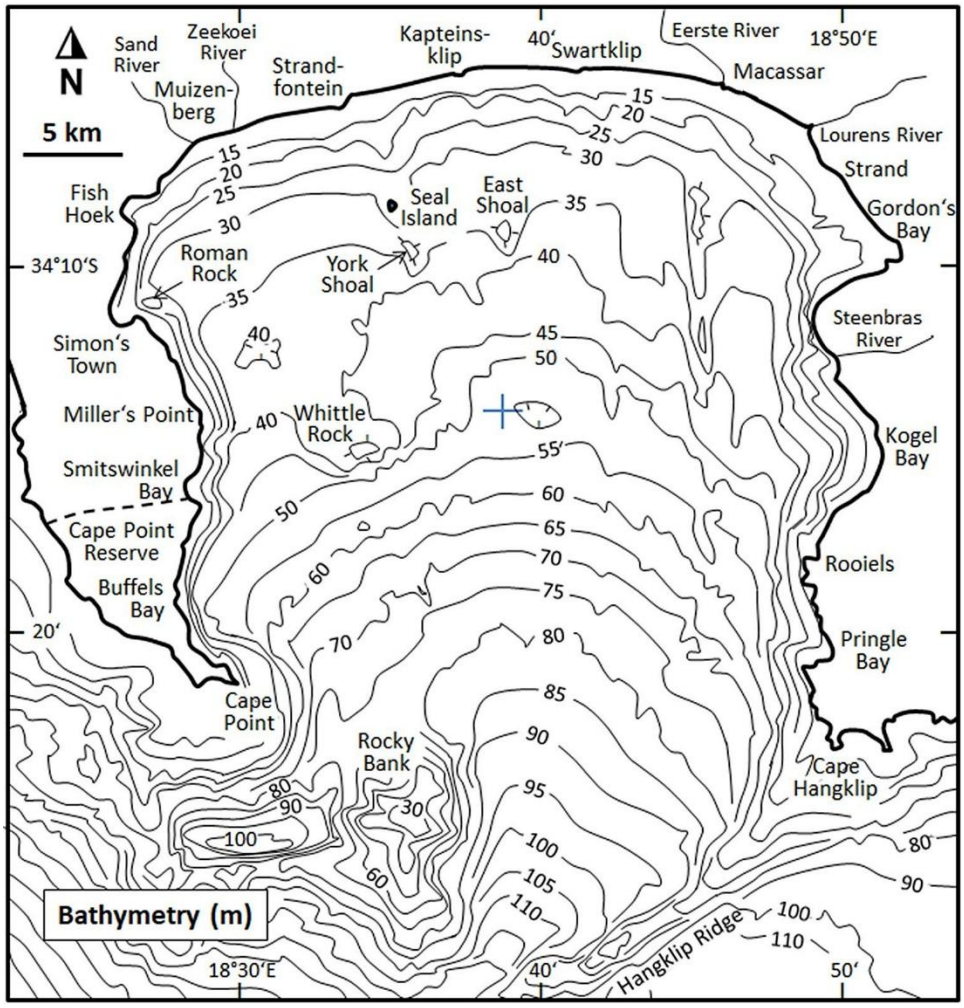

Figure 2) The bathymetry of False Bay and the names of well-known locations and features. The blue cross indicates the centre of the bay (From Flemming, 2024; based on Glass, 1976)

The average depth is ~41 m and the deepest point near the entrance is ~90 m (Taljaard et al., 2000).The bay is open to the sea at its southern extent, which is defined by Cape Point and Cape Hangklip to the west and east respectively. The northern extent is defined by long sweeping beaches separated halfway by the eroding cliffs found from Kapteinsklip to Swartklip.

The boulders and cliffs of the rocky eastern and western shores are interspersed with small sandy beaches. Mountain Group Sandstone and Malmesbury Group Shale (Flemming, 2024).

The bay has been split into four geographical zones which categorize sectors of the bay with similar bathymetric features (Atkins, 1970a). The northern sector is categorized by a gentle slope (~1:400) with a fragmented rocky bottom to the west and a predominantly sandy bottom to the east (Mallory, 1970). The bathymetry on the eastern and western peripheries of the bay is markedly steep (Fig. 1).The west zone is characterized by several large rocky features listed here from north to south: Roman Rock, Seal Island & York Shoal, East Shoal, Whittle Rock and Rocky Bank (Mallory, 1970). These features are a mix of granite and sandstone and form part of the Cape Granite and Table Mountain Group of geological formations (Flemming, 2024). The eastern side is characterized by long N-S running ridges, some of which are ~17 km long and ~300 m wide (Mallory, 1970). These ridges are comprised of shale and form part of the Malmesbury Group (Flemming, 2024). Two distinct terraces, one between 30 and 45 m, the other between 50 and 55 m, exist in the bay and are indicative of Pleistocene (2.6 Ma to 11 700 ka) sea-level stillstands (Flemming, 2024).

Given this pre-historic context, the bay itself can be seen as the southernmost extension of the Cape Flats, a sandy valley which links the Cape Peninsula on the west to the mainland on the east. The eastern side of the bay is rimmed by the mountainous inland terrain of the Hottentots Holland Mountains, with relatively high ranges of between 1100 and 1400 m (Bonnardot et al., 2005). The Cape Peninsula mountain range belts the bay to the west and has a slightly lower range of between 600 and 1100 m (Jury, 1991). The intricate orography of the terrain is shown in Fig 2. The orography controls the wind field over the area under the varying wind regimes and creates wind shadows in the lee of the mountains (Jury, 1991).

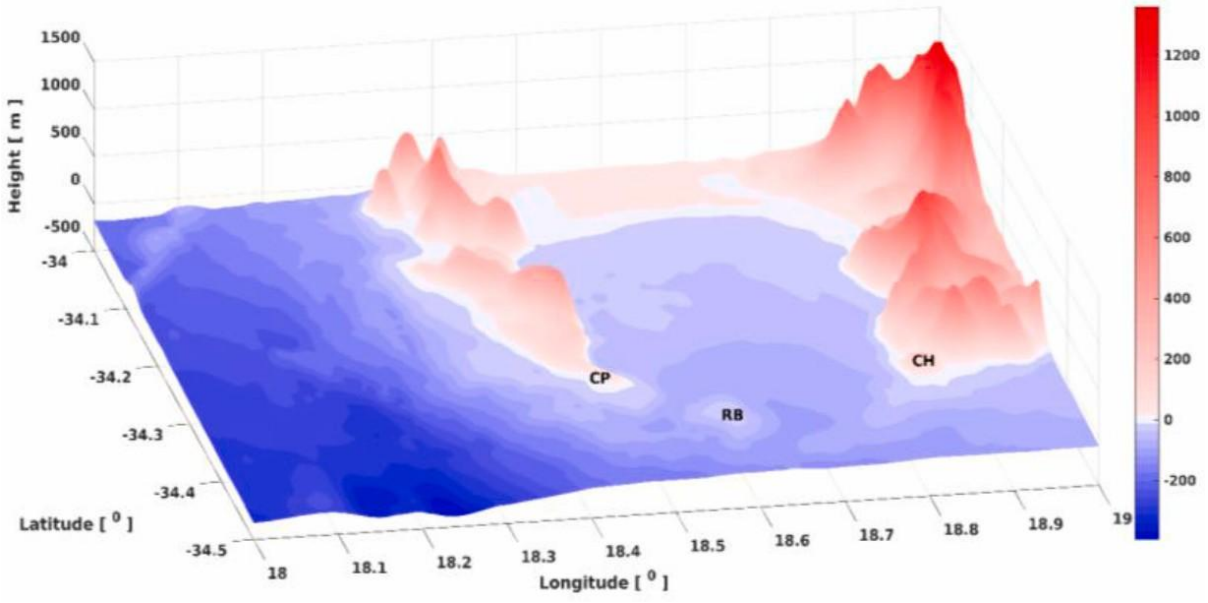

Figure 3) Bathymetry and orography of False Bay. Cape Point (CP), Rocky Bank (RB) and Cape Hangklip (CH) are shown (From Daniels et al., 2022).

3.2 Wind Climate

South African weather is primarily seasonal and dominated by large scale synoptic circulations which result from the interactions between the South Atlantic high pressure cell (SAH) and mid-latitude pressure systems that are associated with the upper-level westerlies. Wind over the

bay is controlled by two main factors, the first being the nature and time scale of synoptic weather systems akin to the region, the second being the orography which leads to orographically sheared winds being common (Gründlingh et al., 1989; Jury et al., 1985) The eastward propagation of atmospheric Rossby waves and associated fronts over the Southern Ocean is the major control on the synoptic systems experienced in False Bay (Gründlingh et al., 1989; MacHutchon, 2006; Wainman et al., 1987).

Several synoptic types exist and help explain general atmospheric circulation along the coast. The SAH guides Southern Ocean fronts north-westward to toward the South African coast (Gründlingh et al., 1989). Approaching cold fronts (Mid-latitude cyclones) can generate coastally trapped low pressure systems on the west coast, which propagate eastward as the front encroaches (Gill, 1977). These coastal lows are associated with warm, often strong, offshore Foehn (Berg) winds leading the system, and cool offshore winds trailing it (Gill, 1977). Cold fronts follow the passage of coastal lows and their approach is associated with north-westerly winds, followed by the rapid incursion of cold high latitude air masses after their passage (Gründlingh et al., 1989; Jury et al., 1985).

Fronts are followed by southerly meridional flow along the pressure gradient west of the cyclone. A ridging SAH follows, leading to strong south-easterly conditions, especially in summer. These dynamics, typically cycle on a weekly basis (5-7 days) and are seasonal in nature (Gründlingh et al., 1989).

Cold fronts and coastal lows are often weaker during summer due to the southward shift of the Inter Tropical Convergence Zone. The opposite is true in winter. Summer cycles are characterised by 3-5 days of southeasterlies, where local orographic effects lead to winds speeds exceeding 30 knots at Cape Point (Le Roux, 1975). The height of the inversion layer (unstable atmospheric layer where temperature increases with height) , and by extension the vertical effect of surface winds, is modulated by the passage of these weather systems and can affect the flow and speed of the winds over the bay (Bonnardot et al., 2005; Daniels et al., 2022; Jury, 1991).

The vertical extent of surface winds reaches a minimum during coastal lows, and can create a wind shadow in the lee of the eastern mountains surrounding False Bay (Jury et al., 1985; Wainman et al., 1987). This is the cause of a pronounced slowdown in winds in the north-east of the bay during June, July and August (Atkins, 1970b).

Cut-off lows (COLs) are a class of low pressure system that cross the South African coast ~11 times a year (Singleton and Reason, 2007). These systems become detached from the main jet stream and therefore move independently, sometimes becoming stationary (Singleton and Reason, 2007). Extreme wave conditions, with significant wave height and peak periods exceeding 10 m and 20 s respectively are associated with COLs (Boyd et al., 2014).

The observed wind field in False Bay is highly variable and complicated. Wainman et al. (1987) analysed time series data from anemometers and found that correlations between stations was poor (< 0.6). The spatially varying wind field over False Bay was described as a synoptic sequence by Jury (1984):

South-west regime: Southwesterlies are associated with the ridging SAH following the passage of a cold front. Due to local orographic effects near Walker Bay (to the east of False Bay) the wind field becomes uniformly southerly and strengthens as the pressure gradients increase (Jury, 1984; Largier et al., 1992). This is illustrated in Fig 3a.

South-east regimes

Deep south-east regime: During southerly meridional flow deep southeasterlies flow over the surrounding mountain ranges and are associated with accelerated winds speeds across the bay, as well as the development of a strong easterly downslope jet in the lee of the Kogelberg mountains. Deep conditions are modified when a low level-level subsidence inversion (descending layer of air is heated as it is compressed near the surface) caps the southeasterlies below the mountain ranges to the east and west. This signals the development of the shallow south-east regime. This is illustrated in Fig 3b.

Shallow south-east regime: The ridging process of the SAH and lowers the height of the inversion layer and consequently blocks the surface wind from flowing over the Hottentots Holland mountain range. The mountain range and inversion constrain the wind to a ~600 m vertical extent, hence shallow, and deflect it seaward (Wainman et al., 1987). As a result of this the surface winds accelerate past Cape Hangklip and a wind shadow develops in the lee of the Helderberg Mountains, which impacts surface circulation near Gordon's Bay (Wainman et al., 1987). The data analysed by Wainman et al. (1987) indicate that these winds entering the bay are deflected (by local orographic effects) to become increasingly southerly. The lowering of the inversion layer and subsequent change in the wind field usually occurs over three days (Jury, 1984; Jury et al., 1985) This process is illustrated in Fig 3c.

North-west regime: Northwesters signal the approach of a cold front after the passage of a coastal low. Flow over the Table Mountain range causes the wind to deflect to become more northerly over False Bay, where it blows uniformly. The winds at the mouth of the bay become

stronger and more north-westerly to westerly due to topographic steering at Cape Point. This is illustrated in Fig 3d.

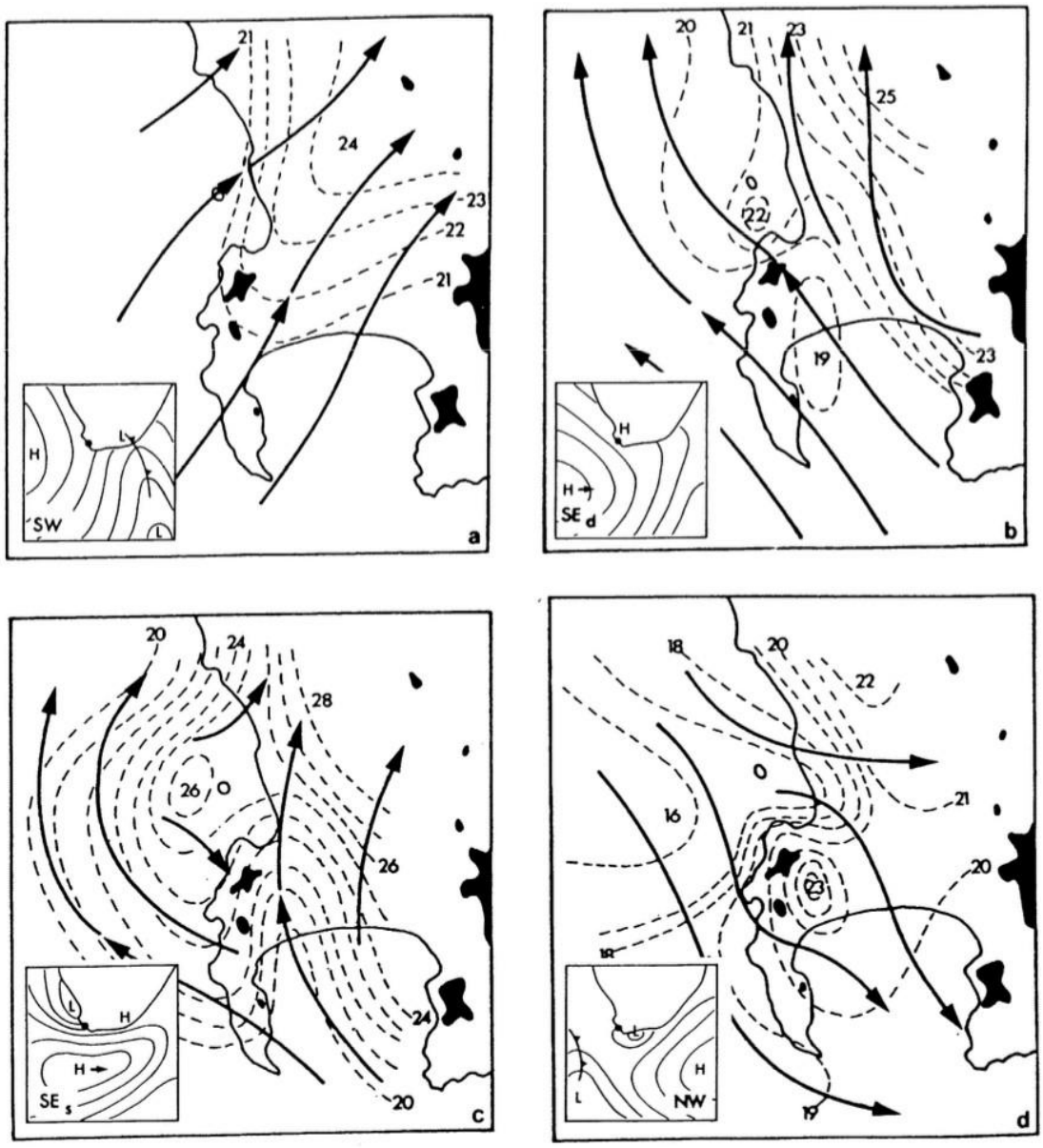

Figure 4) Four wind phases and associated synoptic systems. Southerly meridional flow - a; Ridging SAH - b & c, Coastal low – d. Isobars show truncated values of MSLP in hPa (Jury, 1984).

Fig. 4 shows the 10 m flow streamlines associated with each wind regime and is based on outputs from the South African Weather Service (SAWS) operational Unified Model which has a 4.4 km horizontal grid resolution (Brown et al., 2012; Cullen, 1993). The model output indicates that higher winds speeds are expected over the bay during south-west and deep south-east regimes, compared to slower speeds during the other two regimes. Average wind speed in the bay is~5-7$m \cdot s^{-1}$ according to early observational studies by Le Roux (1975) and Gründlingh et al. (1989). These values correspond well to recent observations (Bonnardot et al., 2005; Daniels et al., 2022) and modelling studies (Coleman, 2019; de Vos, 2022; Salonen, 2019).

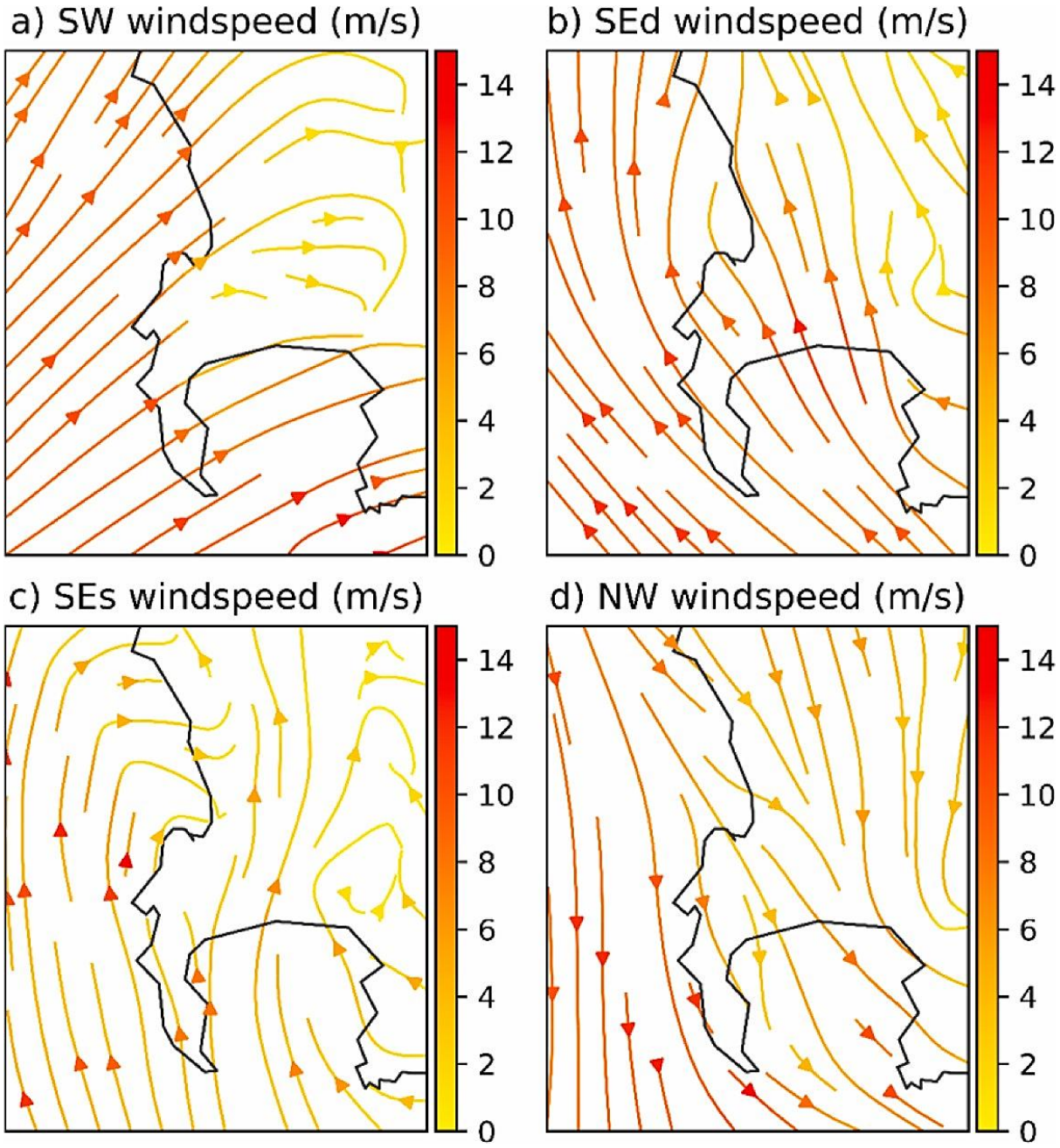

Figure 5) Wind streamlines in $m \cdot s^{-1}$,for the four primary wind regimes that affect False Bay (From Daniels et al, 2022; after Jury, 1987)

3.3 WAVE CLIMATE

Surface ocean waves result from an exchange of energy and momentum between the atmosphere and ocean. These surface waves grow in proportion to wind speed, fetch and duration (Ramos et al., 2021; Salonen, 2019)The wave systems which affect the South African coastline are primarily generated by eastward propagating cold fronts which originate in the South Atlantic and Southern Ocean.(Salonen, 2019; Shillington and Wyndham Harris, 1978). For this reason the predominant swell that affects False Bay comes from the southwest (Shillington and Wyndham Harris, 1978; Shipley, 1964).

The generation zones of swell waves are characterized by a broad wave spectrum (chaotic and spread over a wide range of frequencies and directions). Frequency and directional dispersion processes cause the wave spectrum to narrow, and so organised swell is formed (Veitch et al., 2019). The seasonal cycle of swell affecting False Bay is dependent on the spatio-temporal variability of seasonal cold fronts, which is linked to the seasonal variability of the upper-level westerlies (Taljaard et al., 1969; Veitch et al., 2019).

During austral summer (DJF), wave heights of between 2 and 3 m are normal, but anomalous northward occurrence of cold fronts can lead to larger seas (Joubert, 2008; Massel, 2017). A peak period of between 8 and 16 seconds is associated with the passage of cold fronts to the south of the Cape Point (van Verwolde, 2004).Greater wave heights of between 4 and 5 m are observed in winter months (JJA) (Massel, 2017). Cut-off lows

The Cape Point wave record is a long standing record of wave measurements that affect False Bay, with records split between a buoy at Slangkop (1980-1993) and Cape Point (1994-2010). The Council for Scientific and Industrial Research (CSIR) and Transnet maintained it. Veitch et al. (2018,2019) investigated wave parameters such as significant wave height (H_{m0}) and peak period (T_p) and found a strong seasonal signal. The largest and higher period waves, carrying the most energy, reach the coast during the austral winter months (JJA) and carry a strong westerly component (Veitch et al., 2019).

Veitch et al. (2019) remarked that the seasonal cycle of waves is 'consistent with' the seasonal variation of the amount and depth of cold fronts in the South Atlantic and Atlantic section of the Southern Ocean. The wave generation zone moves closer to South Africa during austral winter due to the northward shift of the upper-level westerlies, leading to the greater observed H_{mo} (Taljaard et al., 1969). Fig 5 shows the wave directions throughout the year with waves from the south-east being dominant(Veitch et al., 2019).

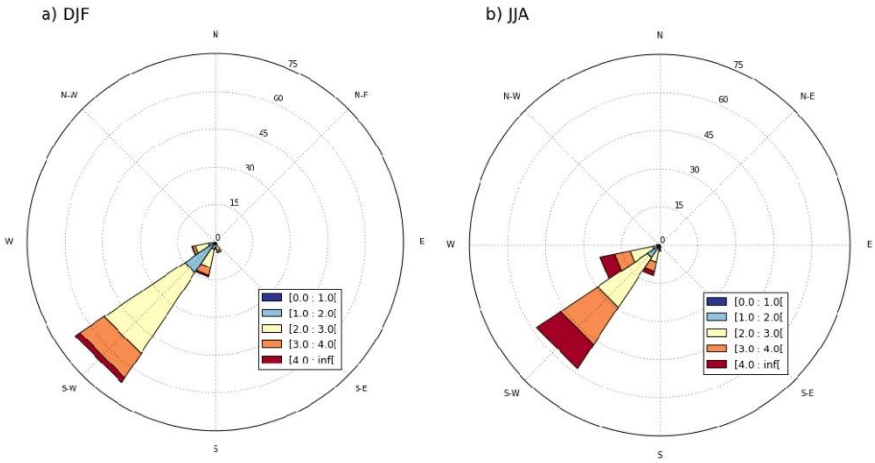

Figure 6) Wave rose showing the observed mean wave direction $(\bar{\theta})$ and significant wave height (H_{m0}) from the Cape Point wave record for the period from 2000 to 2010 (From Veitch et al., 2019).

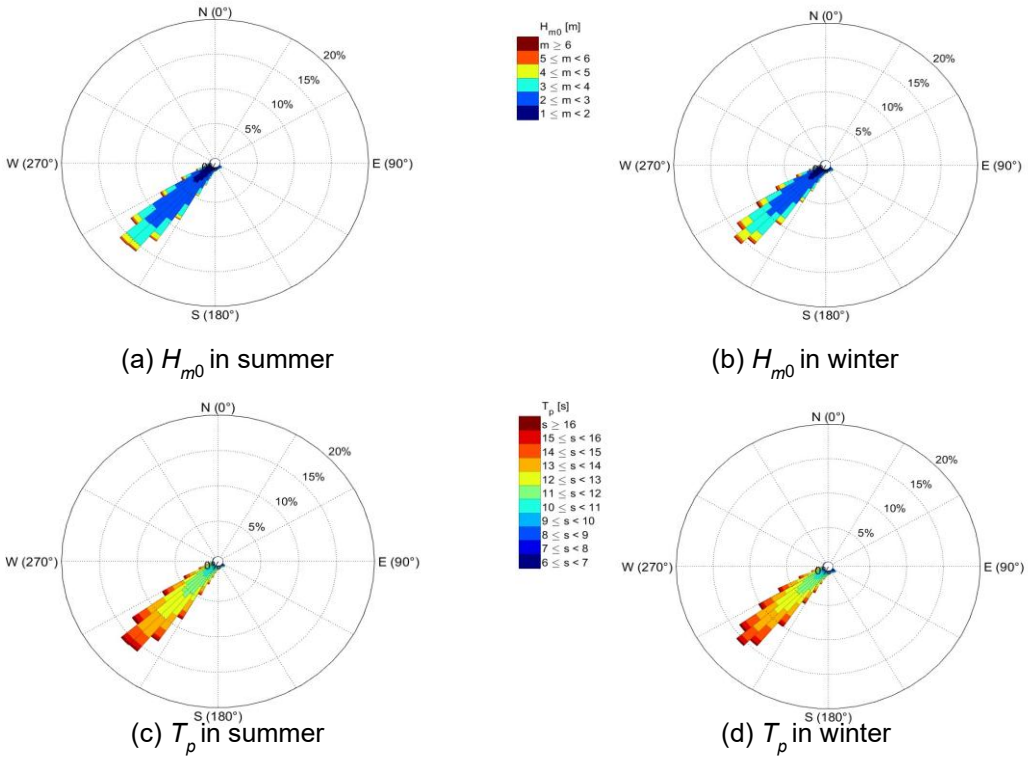

(a) H_{m0} in summer

(b) H_{m0} in winter

(c) T_p in summer

(d) T_p in winter

Figure 7) Seasonal wave roses showing the mean wave directions from the NCEP reanalysis dataset (Kalnay et al., 1996) for a point outside of False Bay $(34.5° S, 18.5 ° E)$. *Significant wave height proportions are shown as percentages are shown by roses a and b, whereas peak period is shown by roses c and d. Each rose shows the proportions associated with* $5°$ *bins (From Salonen, 2019)*

Salonen (2019) generated seasonal wave roses (Fig 6) from the NCEP reanalysis and describes the mean wave direction affecting the bay to be between $210°$ and $240°$ true and the peak periods lie between 11.5 and 13.3 seconds. The observed wave parameters and those derived from the reanalysis product are in general agreement.

The Cape Peninsula shelters the western side of the bay from the predominant south-west swell (Boyd et al., 2014; Salonen, 2019; Shipley, 1964).This blocking of wave energy leads to a nearly 2 m difference between wave heights observed inside and outside of the bay (Boyd et al., 2014). The eastern periphery generally experiences greater wave heights compared to the west (Boyd et al., 2014). Swell entering the bay has long been thought to be influenced by Rocky

Bank, shown in Fig 7 (Shipley, 1946) and Salonen (2019) investigated this with a series of experiments using the Simulating Waves Nearshore (SWAN) model.

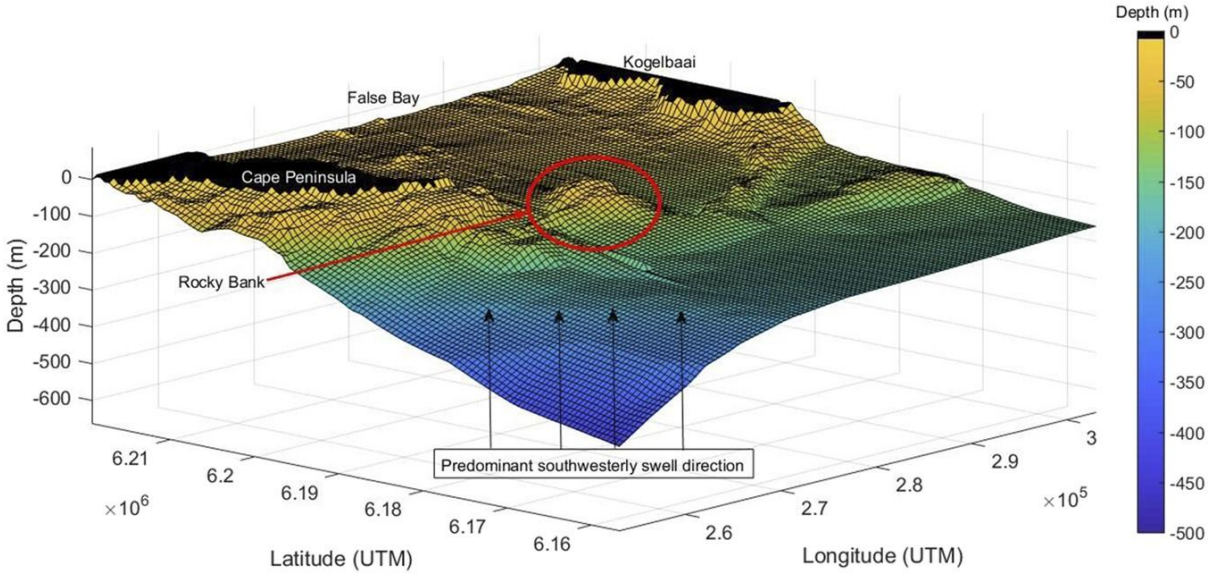

Figure 8) Three-dimensional visualisation of Rocky Bank. The viewing angle is consistent with the predominant swell direction (From Salonen and Rautenbach, 2021)

The main observation was the occurrence of convergent wave energy within the bay due to refraction and spatial focussing caused by Rocky Bank. This leads to an observed reduction in coastal wave heights in the lee of Rocky Bank. The reduction is amplified by increased peak periods. Peak periods greater than 12 seconds lead to a convergent wave refraction pattern and is indicative of the spatial focussing of wave energy by Rocky Bank. Salonen (2019) concluded that the eastern periphery of the bay, known as the "Death Coast" by local anglers, is exposed to the effects of spatial focussing and could experience waves large enough to cause accidents.

The bay is surrounded by local orographic features and semi-sheltered from the incoming swell. The importance of locally wind driven waves within embayments is made clear throughout the literature (Coleman, 2019; Daniels et al., 2022; de Vos, 2022; Jury, 1991; Salonen, 2019). Daniels et al (2022) set up experiments using the SWAN model forced by wind products of various resolutions (to capture orographic effects) to investigate the effects of local winds on waves and currents within the bay. The experiments confirmed that waves on the western periphery are generated by local winds, rather than incoming swell. The eastern periphery is more exposed to the predominant swell, as discussed previously, and the wave field is only marginally influenced by local wind forcing. These findings are attributed to the high resolution wind field provided by the Wind Atlas of South Africa (WASA) product.

3.4 Tides and Inertial Motion

The tidal range in False Bay is approximately 0.8 m and 1.6 m during neap and spring cycles respectively (Gründlingh et al., 1989). The ebb and flood are known generate currents when winds and waves are calm, particularly around the coast and in shallow areas to the north (Atkins, 1970b; Wainman et al., 1987). The co-occurrence of high tides and intense storms are the main contributors to coastal erosion and damage to infrastructure such as railways and beach resorts (Fourie et al., 2015). Historical observations by Atkins (1970b) found that ebb and flood tides modulate currents. Gründlingh et al. (1989) investigated this further by deploying an

array of current meters in the lower half of the water column near the mouth of the bay during the summer of 1986/87 (DJF).

The semi-diurnal tidal constituent was identified as the most significant, especially in the meridional component (N-S), and increased in magnitude from west to east (Gründlingh et al., 1989). The principal axis was in a north-northeast to south-southwest direction (in and out of the bay) with a flow rate of $2.6 - 3.8\ cm \cdot s^{-1}$ (Gründlingh et al., 1989). The diurnal tide had a flow rate of comparable magnitude (Gründlingh et al., 1989) $(2.2 - 3.3\ cm \cdot s^{-1})$, but was more evident in the zonal (E-W) current component (Gründlingh et al., 1989).

A modelling study by Coleman (2019) supported the observation of a decoupling of surface and bottom flows and described bottom flows as weak tidal currents with a magnitude $\leq 10\ cm \cdot s^{-1}$ (Nicholson, 2011). Neap and spring tidal currents were similar under flood and ebb conditions (Coleman, 2019). Flood tidal currents had a typical range of $2 - 10\ cm \cdot s^{-1}$ throughout the bay. They accelerated around Cape Point, over Rocky Bank and along the steep eastern shoreline (Coleman, 2019). Ebb tidal currents had a comparable magnitude range of $2 - 6\ cm \cdot s^{-1}$. Magnitudes reached $10 - 25\ cm \cdot s^{-1}$ around Cape Point and over Rocky Bank.

Inertial motion is a significant and regular variation in the flow of currents caused by the rotation of the Earth. The inertial period is time that it takes a fluid parcel to complete one inertial oscillation.

3.5 LARGE SCALE CLIMATE VARIABILITY

Energy transfers between the ocean and atmosphere are dynamic and involve complex processes that span all spatio-temporal scales (Ramos et al., 2021). Climate oscillations are known to influence sea level pressures as well as wind patterns, which in turn affects surface ocean waves (Hemer et al., 2010; Ramos et al., 2021). Few studies have looked into the role of these oscillations, and their effect on atmospheric circulation in the region of the South Atlantic.

Veitch et al. (2019) investigated the effects of El Niño Southern Oscillation (ENSO) and the Southern Annular Mode (SAM) on the intensity of and adjustment of mid-latitude cyclone tracks (cold fronts). This was paired with data from the Cape Point wave record to elucidate the effect on the wave climate. A positive (negative) ENSO is associated with a positive (negative) sea surface temperature anomaly in the central/eastern tropical Pacific. A positive (negative) SAM is associated with pressure gradient changes between the mid and high latitudes in the southern hemisphere. A positive (negative) westerly wind speed anomaly is associated with a poleward (equatorward) shift in storm tracks. A summary of Veitch et al. (2019)'s findings follow:

Winter (JJA)

The mean wave height was not related to ENSO or SAM. Mean wave direction changes to become more southerly, with a clear shift between 1980-1992 and 1994 -2006. The phase of SAM affected the frequency of extreme wave events, with a reduction (increase) during a positive (negative) SAM.

Summer (DJF)

Waves are smaller and more southerly. A negative (positive) SAM is associated with larger (smaller) more westerly (southerly) waves. A negative (positive) ENSO is associated with

smaller (larger) more southerly (westerly) waves. The co-occurrence of a positive ENSO and negative SAM lead to an increase in westerly wave heights.

3.6 Density Structure

Wind dynamics are the primary driver of the circulation in False Bay, and are therefore seen as the main driver of the vertical temperature structure and stratification of the bay (Atkins, 1970a, 1970b; Dufois and Rouault, 2012; Gründlingh and Largier, 1988; Jury, 1991; Wainman et al., 1987). False Bay is characterized by thermal stratification during summer (DJF) and isothermal during winter (JJA) (Dufois and Rouault, 2012). During summer a temperature differential of $5 - 9\ ^{\circ}C$ is expected between the surface and 50 m water depth (Atkins, 1970a).

Hydrodynamic modelling of False Bay indicates that Rocky Bank segregates warmer western water from colder eastern waters (Coleman, 2019). Bottom waters east of Rocky Bank are consistently (under well-mixed and stratified conditions) approximately 1-2 $^{\circ}C$ colder than to its west (Coleman, 2019). Coleman's (2019) model showed (given stratified conditions) that the north-westerly winds, usually associated with warmer months, cause cold offshore water to be advected into the centre of the bay.

Preferential upwelling on the north-west side of capes is noted by Boyd et al. (1985) at Danger Point (see also Jury op. cit.), Cape Hangklip and Cape Point (Jury 1985)." (Largier et al., 1992, p. 323)

Freshwater input

3.7 Circulation

Four main surface circulation patterns have been observed in False Bay since the early 1970s. The first descriptions by Atkins (1970b) indicate a dominant bimodal circulation dependent on the prevailing wind regime. During weak winds tidal and inertial currents become important. It is important to note that the influence of wave-driven currents is thought to be most important in the shallow regions, especially in the northern sector, with wind-driven currents being dominant in deeper waters. The dominant wind-driven patterns are described below:

South-easterly driven circulation

Previous studies show that south-easterly winds set up a cyclonic (clockwise in the SH) circulation throughout the bay (Fig. 9). The wind shadow in the lee of the Helderberg Mountains allows an anticyclonic circulation to develop near Gordon's Bay (Atkins, 1970b; Coleman, 2019; Taljaard et al., 2000). This is mostly observed during summer months due to the prevailing wind regime. This pattern has been observed (Atkins, 1970b; Gründlingh et al., 1989; Wainman et al., 1987) and modelled (Coleman, 2019; de Vos, 2022; Jacobson, 2014; Nicholson, 2011; Van Foreest and Jury, 1985) multiple times. It is consistent with general north-westward motion with a frequency similar to the south-easterly winds (Wainman et al., 1987). The clockwise motion is partially set up by the bifurcation of a strong west-north-westward flow at the mouth of the bay near Cape Point (Atkins, 1970b; Boyd et al., 2014; Gründlingh et al., 1989; Isaac, 1937; Largier et al., 1992). An equatorward flow is then established along the western shorelines. Cyclonic circulation persists under calm and weaker north-westerly wind conditions. This is likely due to the contribution of wave-driven currents along the northern shoreline, as well as persistent density structures set up by strong southeasterly winds (Atkins, 1970a; CSIR, 1982; Jacobson, 2014). Moddeled current magnitudes are typically $\leq 10\ cm \cdot s^{-1}$ and $\leq 5\ cm \cdot s^{-1}$ at the surface

and seabed respectively (Coleman, 2019).The decopling of surface and bottom flows is consistent with observations (Gründlingh et al., 1989; Wainman et al., 1987). Cyclonic circulation results in the net offshore advection of nearshore waters near Cape Hangklip and the advection of cold offshore waters into the bay near Cape Point (Coleman, 2019).

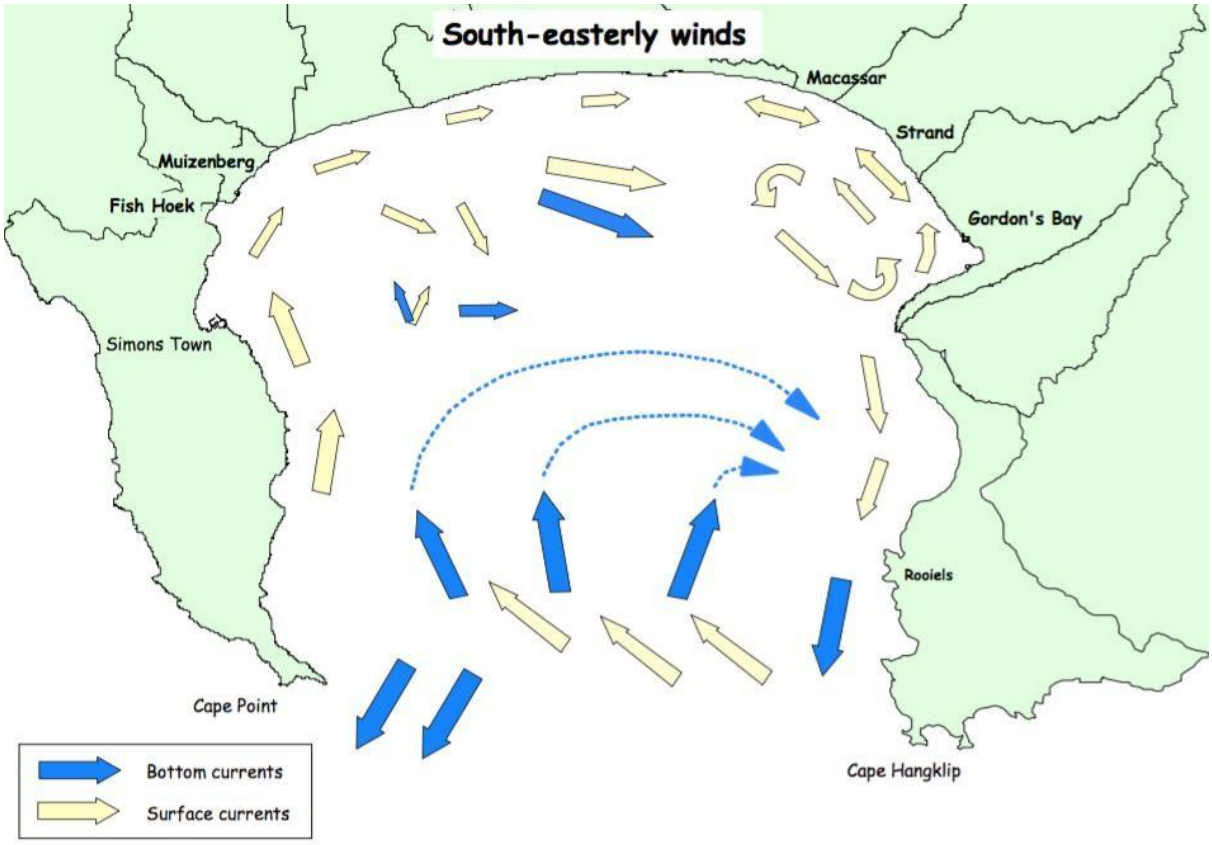

Figure 9a) Schematic of the surface flow and deep-water flow in False Bay under southeasterly wind conditions, inferred from previous observational studies form Taljaard et al. (2000) The dotted arrows indicate weak bottom currents.

North-westerly driven circulation

Observational studies alluded to an anticyclonic (anti-clockwise in the SH) circulation in the bay under north-westerly winds (Atkins, 1970b; CSIR, 1982; Gründlingh et al., 1989; Wainman et al., 1987). A description of the observations follow: North-westerly winds drive an east-north-eastward current near the mouth of the bay (Atkins, 1970b; Wainman et al., 1987). This current is deflected and flows equatorward on the eastern side of the bay (Wainman et al., 1987). This drives the formation of a cyclonic gyre near Gordons Bay (Fig. 10)

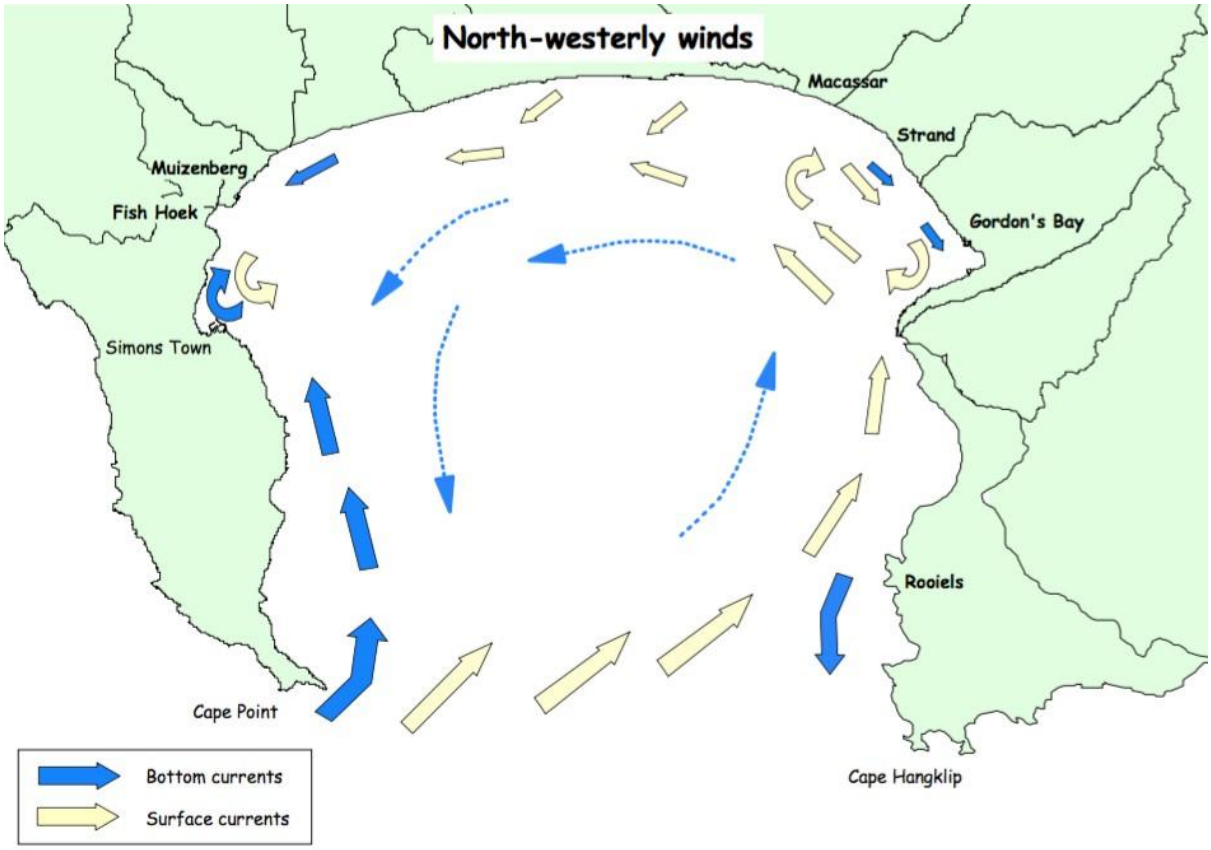

Figure 10) Schematic of the surface flow and deep-water flow in False Bay under north westerly wind conditions, inferred from previous observational studies form Taljaard et al. (2000). The dotted arrows indicate weak bottom currents.

Taljaard et al. (2000) noted that the correlation between a north-westerly wind and the current direction is weaker than the same for a south-easterly wind. A 3D hydrodynamical model by Coleman (2019) used wind forcing, tidal forcing, temperature-depth profiles on the boundary and atmospheric input to model the circulation within False Bay. The model does not feature wave-coupling and therefore does not resolve the circulation within the shallow regions of the bay, especially the northern shores. The model was used to show that the north-westerly winds do not drive the anticyclonic circulation that has been observed, and rather that it results in a spatially-uniform current field within the bay. The explanation given for this is that the wind field over the bay during north-westerly winds is much less complex that that of south-easterly winds (refer to section 3.2). In general, the surface currents in the deeper regions of the bay flow toward the southeast at around $0.3\ \mathrm{m} \cdot \mathrm{s}^{-1}$ (Coleman, 2019). This creates accelerated flows, with speeds up to $0.45\ m \cdot s^{-1}$, around Cape Point, Cape Hangklip and along the eastern shoreline. Surface waters moving out of the bay drives bottom currents to force water from near the entrance to the middle of the bay (Coleman, 2019; Nicholson, 2011). Bottom currents respond to the out-of-bay advection of surface waters by forcing deep water at the entrance of the bay into the centre (Coleman, 2019; Nicholson, 2011). Average bottom current speeds are between 0.05 and $0.10\ m \cdot s^{-1}$ in the centre of the bay but accelerate to approximately $0.30\ m \cdot s^{-1}$ around the headlands and over Rocky Bank (Coleman, 2019).

A more recent study showed that the development of bottom return currents, and subsequent vertical shear, tends to develop during north-north-westerly winds (de Vos, 2022). Anticyclonic

gyre circulation can develop throughout the water column given northerly wind conditions (de Vos, 2022).

Wave-driven currents

The northern shore and shallow areas to the west and east comprises several sandy beaches with a wide surf zone where wave-driven currents and turbulence dominates (CSIR, 1982; Fourie et al., 2015; Salonen, 2019). The direction and magnitude of the currents is governed by the angle of obliquely incident waves and/or wave setup (CSIR, 1982; de Vos, 2022).

Wind-driven surface and bottom currents in False Bay have been observed (Gründlingh et al., 1989) and modelled (Coleman, 2019; Nicholson, 2011) to be decoupled. Surface flows are influenced by the wind, while bottom currents are often in a slightly different direction with a lower magnitude.

The circulation in False Bay is highly dynamic at sub-seasonal to decadal time scales and alternate in nature (Dufois and Rouault, 2012).

4 BIBLIOGRAPHY

Atkins, G.R., 1970a. Thermal Structure and Salinity of False Bay. Trans. R. Soc. South Afr. 39, 117–128. https://doi.org/10.1080/00359197009519107

Atkins, G.R., 1970b. Winds and Current Patterns in False Bay. Trans. R. Soc. South Afr. 39, 139–148. https://doi.org/10.1080/00359197009519109

Bang, N., Andrews, W., 1974. Direct current measurements of a shelf-edge frontal jet in the southern Benguela system. J. Mar. Res. 32.

Bonnardot, V., Planchon, O., Cautenet, S., 2005. Sea breeze development under an offshore synoptic wind in the South-Western Cape and implications for the Stellenbosch wine-producing area. Theor. Appl. Climatol. 81, 203–218. https://doi.org/10.1007/s00704-004-0087-y

Boyd, A., Theron, A., Rossouw, M., Rautenbach, C., Saint, U., Maherry, A., August, M., 2014. Determination of the Inshore wave climate along the South African coast - Phase 1 for Coastal Hazard and Vulnerability Assessment.

Brown, A., Milton, S., Cullen, M., Golding, B., Mitchell, J., Shelly, A., 2012. Unified Modeling and Prediction of Weather and Climate: A 25-Year Journey. https://doi.org/10.1175/BAMS-D-12-00018.1

Burman, J., 1977. The false bay story. Human & Rousseau Publ, Cape Town, Pretoria.

Coleman, F., 2019. The Development and Validation of a Hydrodynamic Model of False Bay (Master of Engineering). Stellenbosch University, South Africa.

CSIR, 1982. Status Report on Pollution in False Bay (CSIR Report No. C/SEA 8241). CSIR, Stellenbosch, South Africa.

Cullen, M.J.P., 1993. The unified forecast/climate model. Meteorological Office, Bracknell.

Daniels, T., Fearon, G., Vilaplana, A., Hewitson, B., Rautenbach, C., 2022. On the importance of wind generated waves in embayments with complex orographic features – A South African case study. Appl. Ocean Res. 128, 103355. https://doi.org/10.1016/j.apor.2022.103355

de Vos, M., 2022. Modelling waves and near-shore circulation around the Cape Peninsula: towards enhanced predictions for South African coastal activities (Doctor of Philosophy). University of Cape Town, South Africa.

Dufois, F., Rouault, M., 2012. Sea surface temperature in False Bay (South Africa): Towards a better understanding of its seasonal and inter-annual variability. Cont. Shelf Res. 43, 24–35. https://doi.org/10.1016/j.csr.2012.04.009

Flemming, B.W., 2024. Sedimentology of False Bay (Western Cape, South Africa): geological background information for the integrated environmental management of a physically confined coastal compartment. J. Coast. Conserv. 28, 1–23. https://doi.org/10.1007/s11852-024-01080-z

Fourie, J.P., Ansorge, I., Backeberg, B., Cawthra, H.C., MacHutchon, M.R., Zyl, F. van, 2015. The influence of wave action on coastal erosion along Monwabisi Beach, Cape Town. South Afr. J. Geomat. 4, 96–109. https://doi.org/10.4314/sajg.v4i2.3

Gill, A.E., 1977. Coastally trapped waves in the atmosphere. Q. J. R. Meteorol. Soc. 103, 431–440.

Goodwin, A.J.H., Peers, B., 1953. Two Caves at Kalk Bay, Cape Peninsula. South Afr. Archaeol. Bull. 8, 59. https://doi.org/10.2307/3887014

Gründlingh, M.L., Hunter, I.T., Potgieter, E., 1989. Bottom currents at the entrance to False Bay, South Africa. Cont. Shelf Res. 9, 1029–1048. https://doi.org/10.1016/0278-4343(89)90056-3

Gründlingh, M.L., Largier, J.L., 1988. Physical oceanography in False Bay: A review. Suid-Afr. Tydskr. Vir Natuurwetenskap En Tegnol. 7, 133–143. https://doi.org/10.4102/satnt.v7i3.914

Hemer, M.A., Church, J.A., Hunter, J.R., 2010. Variability and trends in the directional wave climate of the Southern Hemisphere. Int. J. Climatol. 30, 475–491. https://doi.org/10.1002/joc.1900

Isaac, W.E., 1937. South African Coastal Waters in Relation to Ocean Currents. Geogr. Rev. 27, 651–664. https://doi.org/10.2307/209863

Jacobson, M., 2014. The influence of a spatially varying wind field on the circulation and thermal structure of False Bay during summer: a numerical modelling study (Honours Thesis). University of Cape Town, South Africa.

Joubert, J.R., 2008. An investigation of the wave energy resource on the South African coast, focusing on the spatial distribution of the south west coast. Stellenbosch: University of Stellenbosch.

Jury, M.R., 1991. The weather of False Bay. Trans. R. Soc. South Afr. 47, 401–418.

Jury, M.R., 1984. Wind shear and differential upwelling along the SW tip of Africa. (Ph.D. thesis). University of Cape Town, South Africa.

Jury, M.R., Kamstra, F., Taunton-Clark, J., 1985. Diurnal wind cycles and upwelling off the northern portion of the Cape Peninsula in summer. South Afr. J. Mar. Sci. 3, 1–10. https://doi.org/10.2989/025776185784461216

Largier, J.L., Chapman, P., Peterson, W.T., Swart, V.P., 1992. The western Agulhas Bank: circulation, stratification and ecology. South Afr. J. Mar. Sci. 12, 319–339. https://doi.org/10.2989/02577619209504709

Le Roux, J.J., 1975. Climate of South Africa, Part 1: Surface winds. (Report WB No. 38). South African Weather Bureau, Dept. Transport, South Africa.

MacHutchon, K.R., 2006. The Characterisation of South African Sea Storms (Ph.D. thesis). Stellenbosch University, Stellenbosch: South Africa.

Mallory, J.K., 1970. The Bathymetry and Microrelief of False Bay. Trans. R. Soc. South Afr. 39, 109–112. https://doi.org/10.1080/00359197009519105

Massel, S.R., 2017. Ocean surface waves: their physics and prediction, 3rd ed. World scientific.

Nicholson, S.A., 2011. The circulation and thermal structure of False Bay: a process-oriented numerical modelling and observational study (MSc thesis). University of Cape Town, Cape Town, South Africa.

Pfaff, M.C., Logston, R.C., Raemaekers, S.J.P.N., Hermes, J.C., Blamey, L.K., Cawthra, H.C., Colenbrander, D.R., Crawford, R.J.M., Day, E., du Plessis, N., Elwen, S.H., Fawcett, S.E., Jury, M.R., Karenyi, N., Kerwath, S.E., Kock, A.A., Krug, M., Lamberth, S.J., Omardien, A., Pitcher, G.C., Rautenbach, C., Robinson, T.B., Rouault, M., Ryan, P.G., Shillington, F.A., Sowman, M., Sparks, C.C., Turpie, J.K., van Niekerk, L., Waldron, H.N., Yeld, E.M., Kirkman, S.P., 2019. A synthesis of three decades of socio-ecological change in False Bay, South Africa: setting the scene for multidisciplinary research and management. Elem. Sci. Anthr. 7, 32. https://doi.org/10.1525/elementa.367

Ramos, M.S., Farina, L., Faria, S.H., Li, C., 2021. Relationships between large-scale climate modes and the South Atlantic Ocean wave climate. Prog. Oceanogr. 197, 102660. https://doi.org/10.1016/j.pocean.2021.102660

Salonen, N.M., 2019. Towards Rogue Wave Characterization in False Bay, South Africa.

Shillington, F.A., Wyndham Harris, T.F., 1978. Surface waves near Cape Town and their associated atmospheric pressure distributions over the South Atlantic. Dtsch. Hydrogr. Z. 31, 67–82. https://doi.org/10.1007/BF02227005

Shipley, A.M., 1964. Some aspects of wave refraction in False Bay. South Afr. J. Sci. 60, 115–120. https://doi.org/10.10520/AJA00382353_1513

Singleton, A.T., Reason, C.J.C., 2007. Variability in the characteristics of cut-off low pressure systems over subtropical southern Africa. Int. J. Climatol. 27, 295–310. https://doi.org/10.1002/joc.1399

Taljaard, A.J., Crutcher, A.H., Jenne, A.R., Loon, A.H. van, Center, C.N.W.R., Defense, C.U.S.D. of, 1969. Climate of the Upper Air: Southern Hemisphere: Volume 1: Temperatures, Dew Points, and Heights at Selected Pressure Levels. https://n2t.org/ark:/85065/d7h131fh

Taljaard, S., van Ballegooyen, R., Morant, P., 2000. False Bay Water Quality Review — Volume 2: Specialist Assessments and Inventories of Available Literature and Data (CSIR Report No. ENV-S-C 2000-086/2). Council for Scientific and Industrial Research, Stellenbosch, South Africa.

Van Foreest, D., Jury, M.R., 1985. A numerical model of the wind-driven circulation in False Bay. South Afr. J. Sci. 81, 312–317.

van Verwolde, E., 2004. Characteristics of extreme wave events and the correlation between atmospheric conditions along the South African coast (Master's Thesis). University of Cape Town, South Africa.

Veitch, J., Rautenbach, C., Hermes, J., Reason, C., 2019. The Cape Point wave record, extreme events and the role of large-scale modes of climate variability. J. Mar. Syst. 198, 103185. https://doi.org/10.1016/j.jmarsys.2019.103185

Wainman, C.K., Polito, A., Nelson, G., 1987. Winds and subsurface currents in the False Bay region, South Africa. South Afr. J. Mar. Sci. 5, 337–346. https://doi.org/10.2989/025776187784522423